32nd Annual International Conference of the IEEE EMBS
Buenos Aires, Argentina, August 31 - September 4, 2010

Characterization of Neurologic Injury using Novel Morphological Analysis of Somatosensory Evoked Potentials

Jai Madhok, Shrivats Iyer, Nitish V. Thakor, *Fellow, IEEE*, Anil Maybhate, *Member,* IEEE

***Abstract* - This paper describes an innovative, easy-to-interpret, clinically translatable tool for analysis of Somatosensory Evoked Potentials (SSEPs). Unlike traditional analysis, which involves peak-to-peak amplitude and latency calculation, this method, phase space analysis, analyzes the overall morphology of the SSEP, and includes greater information. The SSEP is plotted in phase space ($\dot{x}$ vs. x), which leads to an approximately spiral curve. The area swept out by this curve is termed the Phase Space Area (PSA). As PSA calculation involves numerical differentiation, we present a comparison of two different approaches to combat noise amplification: finite-window smoothing, and total variation regularization (TVR) of the numerical derivative. These methods are applied to simulated SSEPs. The efficacy of these methods in performing noise-reduction is assessed and compared with ensemble averaging. While TVR gives a reasonably robust approximation of the derivative, Gaussian smoothing of the derivative offers the best trade-off between the number of signal sweeps required to be averaged, close approximation of the SSEP derivative, and optimal estimation of the PSA. We validate this method by analyzing non-characteristic SSEPs that have indistinguishable peaks as is frequently seen in cases of underlying neurologic injury such as hypoxic-ischemic encephalopathy.**

I. INTRODUCTION

Somatosensory Evoked Potentials (SSEPs) are the electrophysiological response of the sensori-motor pathway to peripheral electrical stimulation. SSEPs are commonly used to characterize the response of the central nervous system to conditions such as spinal cord injury, cardiac arrest-induced neurologic injury, and during intra-operative neural monitoring [1-3].

Clinically obtained SSEPs are typically contaminated with biological (electromyogram artifacts, background EEG activity) and electrical noise. Thus, averaging of 100-1000 sweeps [4] is routinely used to enhance the signal-to-noise ratio. After averaging, SSEPs are usually characterized by their peak-to-peak amplitudes and latencies [4, 5]. Variability in these parameters highlights attenuation in transmission of SSEPs and variations in conduction velocity through the CNS and PNS [4] respectively.

Manuscript received April 1, 2010. This work was supported in part by the U.S. National Institutes of Health under Grant RO1 HL071568.

J. Madhok, S. Iyer, and N. V. Thakor are with the Department of Biomedical Engineering, Johns Hopkins University School of Medicine, Baltimore, MD 21205, USA (e-mail: jaimadhok@jhu.edu; siyer@jhu.edu; nitish@jhu.edu)

A. Maybhate is with the Department of Biomedical Engineering, Johns Hopkins University School of Medicine, Baltimore, MD 21205, USA (phone: 443-287-6341; fax: 410-955-1498; email: anil@jhmi.edu)

However, SSEPs obtained in cases of neural injury are frequently characterized by atypical or indistinguishable shapes, absent peaks, or greatly prolonged latencies, which make automated peak-detection a complex problem, often warranting manual inspection by trained personnel.

Recently, we proposed studying SSEPs using a dynamical systems perspective in the phase space or state space [6, 7] in which the signal is plotted against its instantaneous time-derivative. This method incorporates the overall waveform morphology and has the potential to replace traditional methods of SSEP analysis, with higher sensitivity and specificity with regards to neuro-diagnostic monitoring, without requiring manual intervention.

Further, since noise-amplification is an inherent feature of numerical differentiation, we study two different methods to de-noise the numerical derivative: finite-window smoothing and total variation regularization (TVR) [8] of the numerical derivative and compare them with the traditional signal averaging approach best study SSEPs in the phase space.

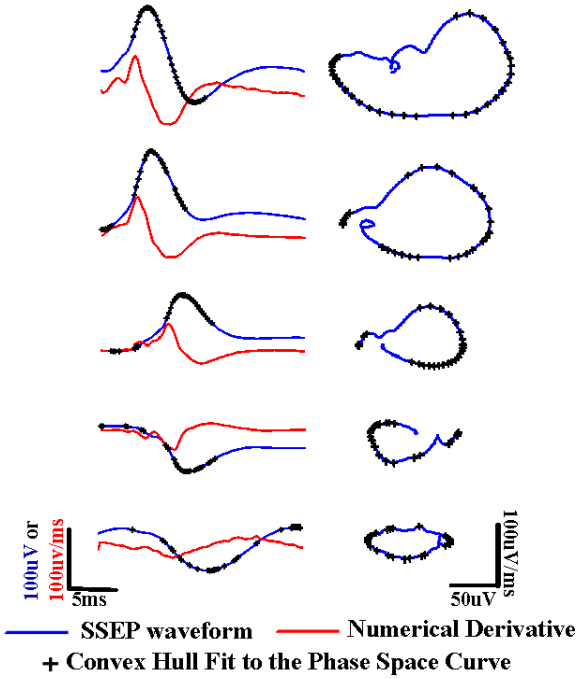

Figure 1: Somatosensory Evoked Potentials (SSEPs) and their representation in the phase space. The left panel represents the SSEP waveforms and their numerical derivatives, and the right panel depicts the phase space transformation of these waveforms. A normal rodent SSEP is shown at the top and as we move down SSEPs recorded during underlying neurologic dysfunction are shown. It is interesting to note that even when peaks becomes less distinguishable or absent during injury, phase space analysis provides a simple, elegant, graphical and quantitative means of describing the waveform

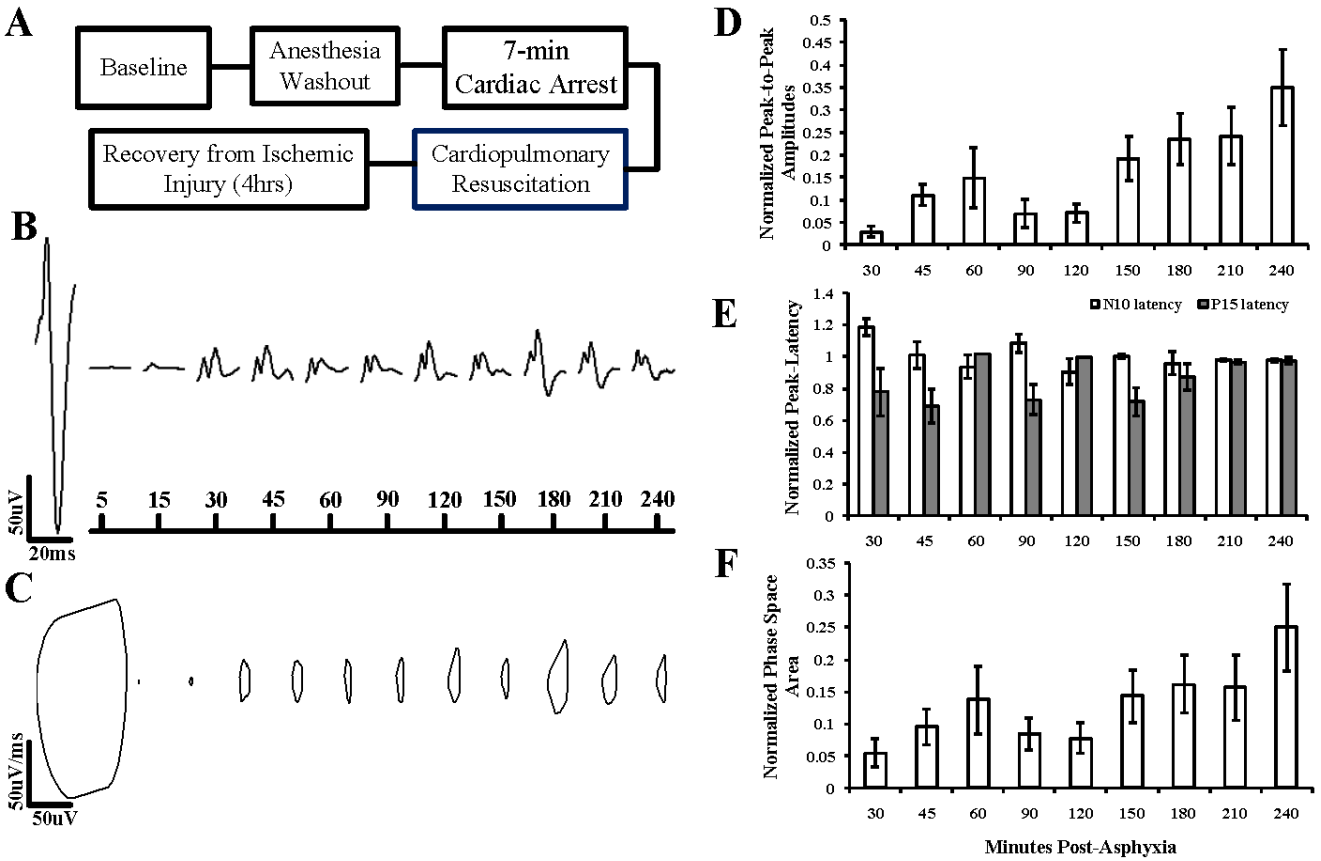

Figure 2: Evaluation of SSEPs after cardiac arrest (CA) induced hypoxic-ischemic injury. A total of 8 rats were subjected to a 7min asphyxial-CA. **(A)** summarizes the experimental protocol used in the study. **(B)** and **(C)** show the recovery of SSEPs and the corresponding convex-hull fits for a representative animal. It is interesting to note the dynamic evolution of SSEPs and how the phase space transformation intuitively captures SSEP recovery. **(D-F)** present a summary of the amplitude-latency and the PSA analysis on the entire cohort. While it is necessary to manually verify the amplitudes and latencies, no such inspection was required for PSA. Further, there were several points at which a amplitude-latency could not be done due to absent peaks.

II. Methods

A. Calculation of the Phase Space Area

Phase-space analysis involves the plotting of the SSEP signal in the $(\dot{x} - x)$ phase plane. The value of $\dot{x}$ is approximated by Newton's Difference Quotient.

$$\dot{x}(t) \approx \frac{\Delta x[n]}{\Delta n} = \frac{x[n + t_s] - x[n]}{t_s};\ t_s = \frac{1}{f_s} \qquad (1)$$

where f_s is the sampling frequency of the signal. The approximately spiral curve that results is known as the phase space curve. In order to compute the area bounded by the PSC, we first fit a convex hull to it. In computational geometry, a convex hull of a set of points P in real vector space is the minimum convex set spanning P. Thus, the convex hull is a simple closed polygon that captures the extent of a non-empty set of points. Several algorithms have been developed to compute the convex hull, and we used the Quickhull algorithm described by Barber, Dobkin, and Huhdanpaa [9]. The two-dimensional area swept out by this curve is termed the Phase Space Area (PSA).

B. Simulation of Somatosensory Evoked Potentials

A template noise-free SSEP sweep was selected from data acquired from the rat somatosensory cortex upon median nerve stimulation of the contralateral forelimb. Since the SSEP was recorded using epidural screw electrodes, it was relatively free of noise. For the purposes of this paper, this SSEP was considered the reference response.

Clinically obtained SSEPs are contaminated with noise that can be approximated to be the sum of two independent components - Gaussian noise, and underlying spontaneous EEG activity. For our simulation, Gaussian noise was generated to be zero-mean, with standard deviation equal to 25% of that of the reference SSEP. EEG noise was generated using a 30th order auto-regressive (AR) model using the Yule-Walker method for parameter estimation. The AR coefficients were obtained using a 10sec long EEG segment also obtained from the same rat as the reference SSEP. These two stochastic components were algebraically summed to the reference to obtain a noisy waveform.

C. Finite-Window Smoothing

The derivative of the noisy SSEP signal was discretely convolved with 3 windows (rectangular, triangular and Gaussian) of variable sizes (N=3, 5, 7, and 9). We determined that a Gaussian window of length 7 was the optimal window for smoothing (data not shown).

D. Total Variation Regularized Differentiation

We apply total variation regularization (TVR) in an attempt to regularize the process of differentiation. As

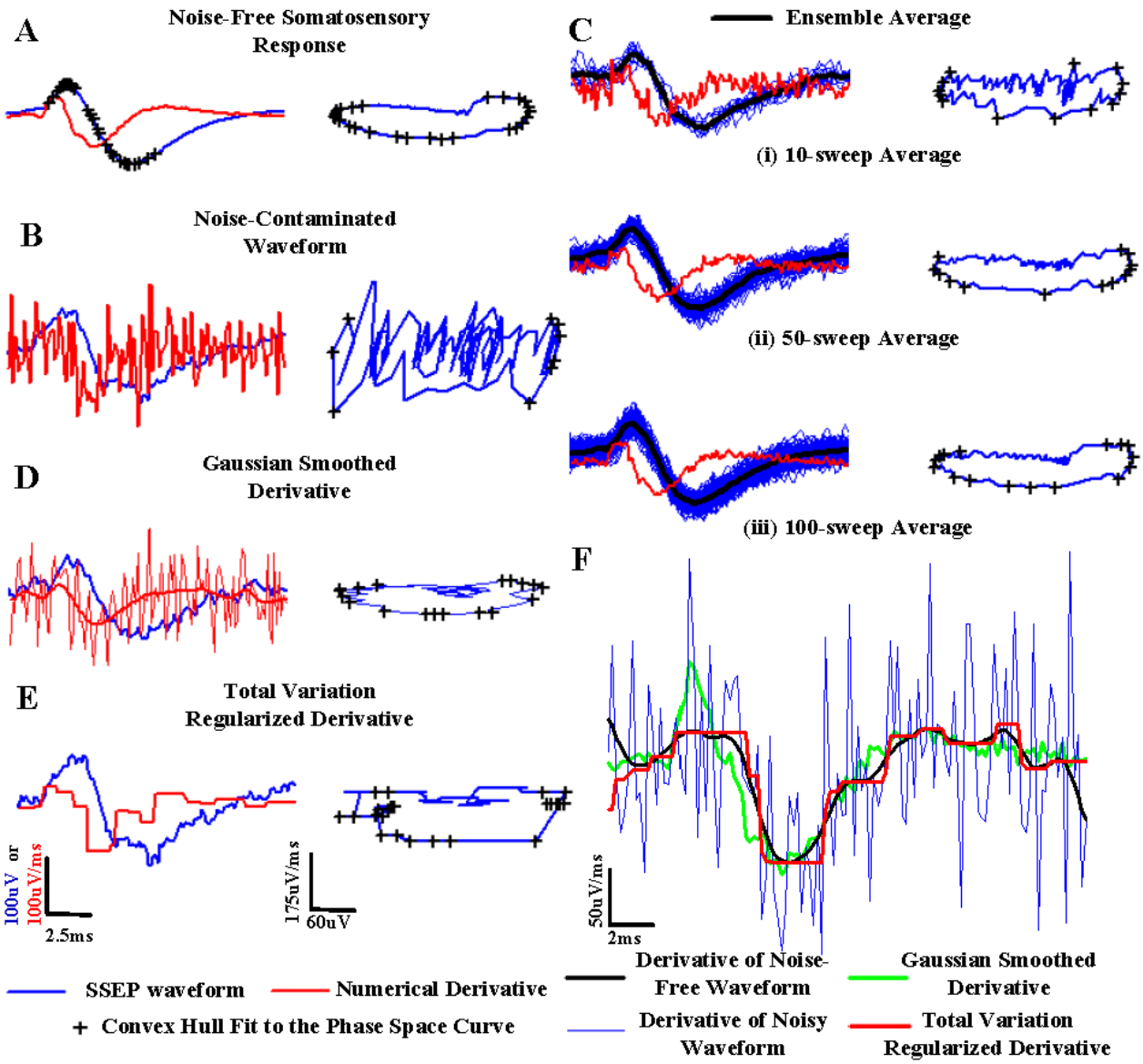

Figure 3: Comparison of different approaches to combat noise-amplification prior to estimation of phase space area (PSA). **(A)** shows the phase space transformation of noise-free somatosensory response. The numerical derivative and the phase space representation become jagged when the SSEP is contaminated with biological and electrical noise **(B)**. To ensure a reasonable estimation of the PSA, stimulus-locked waveforms can be averaged **(C)** or the derivative of a single SSEP sweep maybe smoothed by finite-window convolution **(D)** or the process of numerical differentiation itself maybe restricted **(E)** by using total variation regularization (TVR). **(F)** depicts the effect of these different noise-reduction approaches on the raw numerical derivative. While in this run of the simulation, the TVR-derivative most closely represents the derivative of the reference response, on average the Gaussian smoothed derivation performs better.

described in [8], the total variation regularized derivative of a function *f* is computed as the minimizer of the functional:

$$F(u) = \alpha R(u) + DF(Au - f) \tag{2}$$

where α is the regularization parameter, *R(u)* is the term that penalizes the variability in *u*, *A* is the anti-differentiation operator, and *DF* is the term that penalizes the discrepancy between *Au* and *f* [8]. The regularization parameter α controls the relative penalty on the *irregularity* in *u* and the *discrepancy* between *Au* and *f*. Applying TVR using the above framework and under the assumption that $f \in R^2$ and $f(0) = 0$ on [0, L] we get:

$$F(u) = \alpha \int_0^L |u'| + \frac{1}{2}\int_0^L |Au - f|^2$$

$$where\ Au(x) = \int_0^x u \tag{3}$$

The first term of *F(u)* is the *total variation* of *u'* which for a real-valued function *f* defined on the interval $[0, L] \subset R$ is the one-dimensional arc-length of the curve $(x, f(x))$ for $x \in [0, L]$. The solution that minimizes the functional provides the optimal trade-off between the total variation of the derivative and the error between the estimated anti-derivative and the signal itself. The numerical implementation of this method is described in detail in [8].

III. Results

A. Automated Characterization of Atypical SSEPs

In Fig. 1, we show how the phase space analysis can characterize atypical SSEPs. In the presence of neurologic dysfunction, SSEPs change in unpredictable ways, often resulting in the absence or malformation of characteristic peaks. While traditional methods fail, PSA not only remains calculable, but diminishes with increasing dysfunction, showing that phase space analysis effectively detects changes in signal morphology.

In order to evaluate how PSA performs on real-experimental data, we applied it to SSEPs recorded during the first 4hrs after cardiac arrest (CA) induced hypoxic-ischemic injury. CA results in global neurologic dysfunction and SSEPs are clinically the most reliable marker used for prognosis. However, as shown in Fig. 2(B), the recovery of SSEPs after CA is an unpredictable process, where amplitude-latency analysis would require manual inspection. In contrast, PSA tracks recovery in an unsupervised manner. We show that PSA can accurately track recovery by presenting a comparison of PSA trends with those of amplitudes and latencies in 8 rats subjected to a 7-min asphyxial-CA in Fig. 2(D-F).

B. Performance of Noise-cancellation Approaches in the Estimation of PSA

Fig. 3(A) and (B) together depict the effect that noise in the SSEP can have on calculation of PSA. This validates the incorporation of effective noise-cancellation approaches in the development of phase space analysis. Fig. 2(C) shows that traditional methods of ensemble averaging decrease the error in PSA, but large numbers of sweeps must be acquired for reasonable enhancement of signal-to-noise ratio. Fig. 2(D) shows that Gaussian smoothing can achieve equivalent effects even when applied to a single sweep. In Fig. 2(F) we see that both TVR and Gaussian smoothing can produce reasonable approximations of the reference derivative. The mean-squared errors of the noisy, Gaussian smoothed and total variation regularized derivatives for a 100-iteration simulation are approximately in the ratio: *16:1:2*. Despite this, we see that the step-like nature of the regularized derivative results in a relatively high error in PSA (Fig. 2(E)), with *93:1:2.5* as the corresponding ratio of mean-squared errors.

Table I summarizes these results. For accurate comparison of the different noise-cancellation methods it must be noted that Gaussian smoothing and regularization are performed on a single-sweep.

TABLE I
COMPARISON OF NOISE-CANCELLATION APPROACHES
[a]All errors are with respect to the PSA of the noise-free waveform

Symbol	Normalized Mean-Square Error (%)[a]
Noisy-waveform	640
10-sweep Average	32
50-sweep Average	4.2
100-sweep Average	1.5
Single-sweep Gaussian Smoothed Derivative	7.2
Single-sweep Regularized Derivative	29

IV. Discussion

The phase space analysis of SSEPs provides a number of unique benefits. In particular, it provides an automated, simple, graphical and quantitative tool for characterization. PSA is a single number that can track unexpected and hard-to-interpret changes in waveform morphology.

Vulnerability to noise is the major limitation in application of this method in the clinical setting. It was found that Gaussian smoothing leads to effective de-noising of the derivative without the need for averaging hundreds of sweeps. However, excessive smoothing with either long windows or multiple convolutions with the same window can result in significant attenuation of derivative and/or prolongation of peak latencies. If the smoothing parameters are kept constant, this attenuation is equivalent to a scaling factor and can be disregarded. Any artifactual prolongation of peak latencies is minimal will not affect the PSA as inter-peak latencies are unaffected. While TVR is effective in estimating the derivative, it leads to a coarse approximation of PSA due to step-like nature of the regularized derivative.

Depending upon the experimental conditions and requirements, smoothing or TVR of the derivative will allow for single-sweep or minimally-averaged SSEPs for analysis.

V. Conclusion

The methods described in this paper allow for automated characterization of evoked potentials, capture waveform morphology, and enable analysis with minimal averaging. The ease of implementation of the algorithms described allows for their real-time incorporation in neuro-monitoring systems, and enables their clinical translation.

VI. Acknowledgment

The authors would like to thank Dr. Rick Chartrand for providing us the MATLAB code to implement TVR.

VII. References

[1] S. C. Jones, R. Fernau, and B. L. Woeltjen, "Use of somatosensory evoked potentials to detect peripheral ischemia and potential injury resulting from positioning of the surgical patient: case reports and discussion," *Spine J,* vol. 4, pp. 360-2, May-Jun 2004.

[2] A. All, G. Agrawal, Y. Berrocal, et al., "Characterization of Somatosensory Evoked Potentials for Graded MASCIS Contusion Spinal Cord Injury," *Brain Research,* vol. submitted, 2008.

[3] K. H. Chiappa, *Evoked Potentials in Clinical Medicine*: Lippincott Williams & Wilkins, 1997.

[4] T. F. Karl E. Misulis, *Spehlmann's Evoked Potential Primer* vol. Third Edition, 2001.

[5] M. R. Nuwer, "Fundamentals of evoked potentials and common clinical applications today," *Electroencephalography and clinical neurophysiology,* vol. 106, pp. 142-148, 1998.

[6] J. Madhok, A. Maybhate, W. Xiong, et al., "Quantitative Assessment of Somatosensory Evoked Potentials after Cardiac Arrest in Rats: Prognostication of Functional Outcomes," *Manuscript Under Review at Critical Care Medicine,* 2010.

[7] A. Maybhate, S. Iyer, D. Kerr, et al., "Phase Space Area of Somatosensory Evoked Potentials: A novel marker for monitoring spinal cord injury," *Preprint* 2010.

[8] R. Chartrand, "Numerical differentiation of noisy, nonsmooth data," December 13, 2005.

[9] D. P. D. C. Bradford Barber , Hannu Huhdanpaa, "The Quickhull algorithm for Convex Hulls," *ACM Transactions on Mathematical Software,* vol. 22, pp. 469-483, 1995.